

AD-A088 212

INDIANA UNIV AT BLOOMINGTON DEPT OF CHEMISTRY

F/G 21/2

REDUCTION OF SPECTRAL INTERFERENCES IN FLAME EMISSION SPECTROMETRY-ETC(U)

JUL 80 S W DOWNEY, J G SHABUSHNIG

N00014-76-C-0838

UNCLASSIFIED

TR-27

NL

1 of 1

AD-A

1

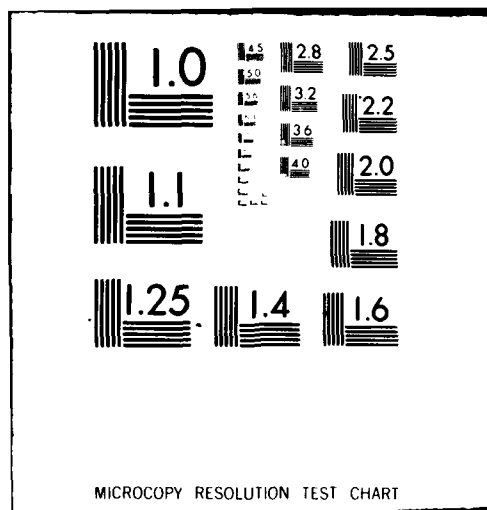
END

DATE

FILED

9-80

DTIC



AD A088212

DDC FILE COPY

UNCLASSIFIED  
SECURITY CLASSIFICATION OF THIS PAGE (When Data Entered)

REPORT DOCUMENTATION PAGE		READ INSTRUCTIONS BEFORE COMPLETING FORM
1. REPORT NUMBER TWENTY-SEVEN	2. GOVT ACCESSION NO. AD-A088212	3. RECIPIENT'S CATALOG NUMBER
4. TITLE (and Subtitle) Reduction of Spectral Interferences in Flame Emission Spectrometry by Selective Spectral-Line Modulation.		5. TYPE OF REPORT & PERIOD COVERED Interim Technical Report.
7. AUTHOR(s) S. W. Downey, J. G. Shabushnig, and G. M. Hieftje		6. PERFORMING ORG. REPORT NUMBER 34
9. PERFORMING ORGANIZATION NAME AND ADDRESS Department of Chemistry Indiana University Bloomington, Indiana 47405		8. CONTRACT OR GRANT NUMBER(s) N-14-76-C-0838
11. CONTROLLING OFFICE NAME AND ADDRESS Office of Naval Research Washington, D.C.		10. PROGRAM ELEMENT, PROJECT, TASK AREA & WORK UNIT NUMBERS NR 51-622
14. MONITORING AGENCY NAME & ADDRESS (if different from Controlling Office)		12. REPORT DATE July 18, 1980
		13. NUMBER OF PAGES 23
		15. SECURITY CLASS. (of this report) UNCLASSIFIED
		16a. DECLASSIFICATION/DOWNGRADING SCHEDULE
16. DISTRIBUTION STATEMENT (of this Report) Approved for public release; distribution unlimited		
17. DISTRIBUTION STATEMENT (of the abstract entered in Block 20, if different from Report)		
18. SUPPLEMENTARY NOTES Prepared for publication in "ANALYTICA CHIMICA ACTA"		
19. KEY WORDS (Continue on reverse side if necessary and identify by block number)		
20. ABSTRACT (Continue on reverse side if necessary and identify by block number) Spectral interferences in flame emission spectrometry have been significantly reduced through the use of selective spectral-line modulation (SLM). In this method, a mirrored, rotating chopper is used to direct the emission from a sample flame alternately through and around a second (modulating) flame; selective modulation is achieved when the modulating flame contains absorbing atoms identical to emitting analyte atoms in the sample flame. In this paper, the effect of optical configuration and modulating conditions		

DD FORM 1 JAN 73 1473

EDITION OF 1 NOV 65 IS OBSOLETE  
S/N 0102-014-6601UNCLASSIFIED  
SECURITY CLASSIFICATION OF THIS PAGE (When Data Entered)

80 3 22

043

OFFICE OF NAVAL RESEARCH

Contract N14-76-C-0838

Task No. NF 051-622

TECHNICAL REPORT NO. 27

REDUCTION OF SPECTRAL INTERFERENCES IN  
FLAME EMISSION SPECTROMETRY BY SELECTIVE  
SPECTRAL-LINE MODULATION

by

S. W. Downey, J. G. Shabushnig, and G. M. Hieftje

Prepared for Publication

in

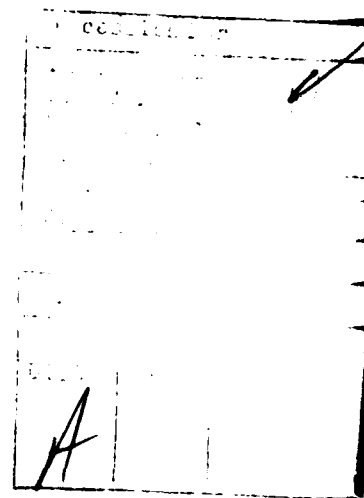
ANALYTICA CHIMICA ACTA

Indiana University

Department of Chemistry

Bloomington, Indiana 47405

July 18, 1980



Reproduction in whole or in part is permitted for  
any purpose of the United States Government

Approved for Public Release; Distribution Unlimited

20. Abstract (continued)

on working curve slope, linearity and signal-to-noise ratio is examined. Also, the ability of SLM to minimize broad-band and narrow-line spectral interferences is demonstrated. In particular, it has been shown that the interference of the 550 nm CaOH band on barium determinations can be largely overcome. Also, interference of several Pd lines on Ni in the 350 nm region can be reduced by SLM. Finally, it is shown how the interference of flame background itself can be restricted in SLM procedures.

1

Atomic emission spectrometry (AES) is becoming the technique of choice for rapid simultaneous or sequential multi-elemental analysis. Unfortunately, AES is often plagued with spectral interference problems, unless scanning high-resolution spectral dispersing systems are employed. These interferences can take several forms and arise from various sources. Overlapping spectral lines from the source background or matrix concomitants and scattered light are commonly encountered spectral interferences.

Even in recent AES instruments (1-3), spectral interferences can be troublesome, subtle and difficult to overcome (4). The most straightforward approach to minimize spectral interferences is to use a high-resolution spectrometer. Unfortunately, this solution is costly and often accompanied by a loss in optical speed. Also, identifying and locking onto the correct spectral line can be difficult in high-resolution work, especially if the source or matrix produces complex background spectra.

Selective modulation can also serve to minimize spectral interferences and avoids many of the limitations of the high-resolution approach. In this scheme, analyte radiation alone is modulated while all other spectral components remain unaffected. Synchronized detection of the modulated signal then rejects interfering radiation.

One form of selective modulation utilizes a periodically interrupted sample introduction system (5,6). This interruption causes emission from the solvent and source to be continuously present at the detector whereas analyte emission is present only at the frequency of sample alternation. Interfering radiation is suppressed when the signal is demodulated. Unfortunately, this

form of selective modulation discriminates against only source background radiation and not that produced by sample components.

Wavelength modulation and derivative spectrometry, another form of selective modulation, have also been used to reduce spectral interferences in AES (7). In this approach, the rapid change in slope of a sharp spectral peak can be detected against the presence of a broadband spectral interferent.

Selective spectral line selection was first achieved in 1954 by Alkemade and Milatz by using a flame as a selective wavelength absorber (8). Other types of atom reservoirs have also been used to modulate selected spectral lines that can then be detected preferentially in the presence of spectral interferences (9,10).

Selective spectral-line modulation (SLM) has been studied further and used in this laboratory to increase the slope and linearity of working curves in continuum source atomic absorption flame spectrometry (11,12). Modulation of the analytical absorption line provided added effective resolution for the 0.35 m monochromator used, thus increasing the working curve slope and linearity.

In the present work, an AES-SLM system similar to that of Alkemade and Milatz (8) was constructed and tested with updated flames and modern detection equipment (cf. Figure 1). Two flames were used, one acting as the emission source, the other serving as the selective spectral line modulator. Radiation emitted from the source flame is alternately directed through and around the modulating flame by a dual-beam optical system; a net difference in intensities between the two beams is then caused by the selective absorption that occurs in the modulating flame. Signals derived from radiation in this selected spectral region are therefore a.c. in nature and can be de-

tected in the presence of the d.c. radiation located outside the narrow region by frequency-selective detection.

The analytical working curves produced by the AES-SLM process were found to be linear, and the sensitivity and signal-to-noise ratio are dependent on modulating solution concentration. At least three types of spectral interferences can be reduced using SLM; broad-band and narrow-line concomitants and source background. The interferences overcome by SLM in this work are the CaOH band overlap of the 553 nm line of Ba, closely spaced Pd and Ni lines near 350 nm and the  $N_2O/C_2H_2$  flame background.

#### EXPERIMENTAL

A schematic diagram of the AES-SLM system used in this work is shown in Figure 1. Details concerning the individual components are summarized in Table 1. In the system, the sample flame is imaged by  $L_1$  into the center of the modulating flame, just above the primary combustion region, and again by  $L_2$  at the monochromator entrance slit. The rotating sector mirror and beam combiner produce the double-beam operation necessary for SLM use. A variable beam attenuator is used to compensate differences in optical throughput between the two beam paths (path B was brighter throughout this work). A basic improvement in design of the system over that described in (12) is the position of the chopper. Here, any emission from the modulating flame will be at a constant level and suppressed by a.c. detection.

The two beams in the AES-SLM system must be completely balanced to avoid false SLM signals. Imbalances can arise from either path throughput differences or spatial inhomogeneities in either beam: the first source of imbalance can be corrected using the variable beam attenuator, while the second can only be



overcome through careful optical design.

The importance of this second, more insidious problem was especially evident when a non-homogeneous (swiss cheese) beam combiner was used. In such an optical element, the substrate is coated with a 50% matrix of small reflective dots, such that half the incident light is reflected. The resulting discrete regions of reflective and transparent surface are highly sensitive to beam wander and inhomogeneity and produced drastically changing relative beam intensities as wavelength was scanned. Of course, for fixed wavelength work, any kind of beam recombination optics can be used, but for multiwavelength applications, a homogeneous combiner is superior. Even with spatially homogeneous optics, small differences in spectral transmission and reflection can create artificial beam imbalances over broad wavelength ranges, and must be overcome through proper calibration.

Optimal modulating solution concentrations were determined from detected signal-to-noise ratios (S/N) at various sample solution concentrations. The S/N was determined in the manner suggested by St. John, et al. (13).

Three spectral interferences were studied using the AES-SLM system. The barium resonance line at 553.5 nm suffers interference from the band emission of CaOH, whose maximum is at 554.0 nm. Wavelength modulation has been shown to be effective in reducing this interference (7) and enables a useful comparison between the methods to be made.

A palladium-nickel mixture will produce two sets of lines that fall within the spectral bandpass of a medium-resolution monochromator. The Pd 351.69 nm and the 351.50 nm Ni line will overlap, as will the Pd 346.077 nm and Ni 346.165 nm lines. Finally, the  $N_2O/C_2H_2$  flame background can also be a major spectral interferent, especially around 380 nm, where the CN bands are located.

Conventional emission spectra of these three interference systems were obtained with the lock-in detection system by blocking entirely the path through the modulating flame. This approach provides the desired detection mode and enables the same optical system to be used, so that an appropriate comparison can be made.

All stock solutions were prepared as described by Dean and Rains (14) using reagent grade metals, salts and acids. For the Ca/Ba interference study, all solutions contained 1000  $\mu\text{g/mL}$  potassium as an ionization suppressant.

## RESULTS AND DISCUSSION

Effect of Modulating Solution Concentration. Figure 2 reveals the influence of modulating solution concentration on working curve slope and linearity. Understandably, all curves show good linearity over the concentration range studied and the slope of the curves are greater at higher modulating solution concentrations.

The practical upper limit to modulating solution concentration will vary from element to element and will be dictated by the amount of noise generated by emission from the modulating element and by concentration-related line broadening effects. In continuum-source AA, such line broadening limits SLM sensitivity and linearity (11,12). Here, however; the analyte emission line is about the same width as the modulating absorption line, so modulation of background continuum is not a severe performance-reducing problem.

Although not evident over the concentration ranges shown in Figure 2, AES-SLM working curves exhibit self-absorption-caused non-linearity at high sample concentrations, just as do other flame emission methods.

A far more important criterion than linearity for selecting optimal modulating conditions is the signal-to-noise ratio. Although the present SLM system does not respond directly to emission from the modulating flame, the shot noise such emission generates can still be a problem and, for some elements, can dominate at high modulating solution concentrations. Moreover, modulating-flame-based flicker noise will further degrade S/N for any element.

In Figure 3, the decrease in S/N at high modulating solution concentrations is due to both a substantial noise increase and small signal increase. Obviously, compromises must be made to achieve optimal modulating conditions and optimal conditions will vary. Understandably, strongly emitting elements will have lower optimal modulating concentrations while weaker emitters can have higher modulating concentrations.

A further complication of the use of high modulation solution concentrations is salt buildup in the modulating nebulizer and burner.

Other Noise Sources. Noise generated by the chopper is especially troublesome, for the chopper defines the modulating frequency (12). Any roughness or other inhomogeneity present over a small portion of the chopper's mirrored surface can add a significant amount of noise to the SLM signal. The rotation of the heavy chopper itself can upset the system through mechanical vibration and the generation of air currents which flutter the flames at the chopper frequency.

The chopper frequency (30 Hz) itself increased the system noise in the present device. For example, the mercury 546.0 nm line from room illumination was found to produce a false signal with just the detection electronics in operation. Later work, with a different modulation frequency (13.7 Hz) alleviated this problem.

Flicker noise sources are minimized in this SLM system but are still present. The position of the modulating flame prevents the modulation of any background flicker noise originating there. However, any flicker of the absorption analyte line is multiplicative and would appear as a detected fluctuation in the selective attenuation. Conveniently, source-flame-based flicker noise is modulated only over the bandwidth of the modulating atoms and not over the entire spectral bandpass of the spectrometer, thereby reducing its effect. This situation is in contrast to previous SLM work (12) where the chopper position produced modulation of the emission from the modulating flame.

Reduction of Spectral Interferences. Figure 4A shows a portion of the conventional emission spectrum of a solution containing 10  $\mu\text{g/mL}$  Ca and 20  $\mu\text{g/mL}$  Ba: Figure 4B shows the Ba-selective AES-SLM scan of the same sample. Clearly, the SLM procedure has essentially overcome interference from the Ca band. Significantly, in the SLM technique, the resolution is not determined by the monochromator, so high optical throughput need not be sacrificed to obtain high effective resolution.

The results seen in Figure 4 compare very favorably with those produced by wavelength modulation (7). Both techniques are able to reject unwanted contributions to the analytical signal from broad background sources. In SLM, however, a small portion of the background is modulated and detected, specifically that portion of background within the modulator bandpass. Here, the bandpass is approximately 0.05  $\text{\AA}$ , resulting in a small but finite background contribution.

The ability of SLM to reject increasing amounts of interfering radiation is illustrated by Figure 5. The SLM signal at 553.5 nm from a fixed barium concentration (10  $\mu\text{g/mL}$ ) is shown to be nearly immune to large amounts of interfering radiation. The practical limit on the amount of excess radiation

that can be tolerated by SLM is governed by both the residual background modulation discussed above and by shot noise the background generates. The first of these limitations is manifested in Figure 5 as the slight upward curvature of the plot. The second limitation is similar to that which restricts modulating solution concentrations (cf. Figure 3).

Also evident in Figure 5 is a difference in intensity between the AES and AES-SLM signals of a 10  $\mu\text{g/mL}$  Ba solution alone. This difference arises because the SLM method does not result in total modulation of the analyte line; to do so would require an infinite atom concentration in the modulating flame. As a consequence of this reduced signal and the higher noise level in SLM discussed earlier, the SLM approach is somewhat less sensitive than conventional emission measurements.

As a further illustration of the ability of SLM to overcome spectral interferences, consider the Pd 351.69 nm and Ni 351.50 nm lines. As shown in the spectral scan of Figure 6B, these lines appear as an unresolved doublet in a conventional AES measurement using the moderate resolution monochromator employed here. In contrast, a Ni-selective SLM scan (Figure 6A) results in a significant reduction of all Pd features. Specifically, the Pd 348.1 and 351.69 nm lines have been greatly reduced and the Ni lines at 351.50 and 346.16 nm are better resolved.

Significantly, the Ni features of Figure 6 cannot be reduced using Pd as the modulating solution. All of the Pd lines that appear in Figure 6 are the more energetic, nonresonance lines whose lower levels are not sufficiently populated in the air/C<sub>2</sub>H<sub>2</sub> modulating flame used here to produce significant selective modulation. With Pd alone in the modulating solution, the spectral region of Figure 6 appears to be featureless.

In the reduction of line interferences (cf. Figure 6), SLM should prove

superior to wavelength modulation. In the latter method, the resolution of the AES system is still determined by the monochromator whereas in SLM the effective resolution is that of an atomic absorption linewidth.

Figure 7 illustrates the ability of SLM to overcome spectral interference from source background. Figure 7A shows a conventional scan of the  $\text{N}_2\text{O}/\text{C}_2\text{H}_2$  flame's background between 320 and 490 nm. The intense CN band at 390 nm is the major feature. The CN band is greatly reduced in the AES-SLM spectrum (Figure 7B).

Of course, not all background features will be removed by SLM. The two flames used here ( $\text{air}/\text{C}_2\text{H}_2$  and  $\text{N}_2\text{O}/\text{C}_2\text{H}_2$ ) have some species in common, e.g. OH, and these will experience some modulation. In the spectral region shown in Figure 7, however, it is seen that these common species have little effect.

#### CONCLUSION

It is important in SLM that the excitation atom reservoir is at a higher temperature than the modulating atom reservoir. If the temperatures were equal, no net absorption or emission would occur, and no SLM signal would be seen. This factor limits the choice of modulating flame or other atom reservoirs to those which are relatively cool and therefore exhibit poor atomization efficiency for some elements. This situation might restrict SLM to the determination of only selected elements or combinations of elements. Moreover, because ions are not in high concentrations in most flames, the SLM measurement of ion lines will be difficult or will require alternative selective absorption cells. This factor might preclude the useful application of SLM to plasma emission.

The SLM concept should also be applicable to nondispersive detection. Although such an application would suffer an increase in noise level, spectral

interference should be minimized since effective isolation of the analytical line occurs prior to detection.

Work is currently underway in our laboratories to apply SLM to other analyte and matrix combinations and to other sources (e.g. ICP) where source background, overlapping lines, stray light, and other spectral interferences limit analytical attractiveness.

CREDIT  
~~XXXX~~

Supported in part by the Office of Naval Research and by the National Science Foundation through grant CHE 79-18073.

## REFERENCES

1. G. W. Johnson, H. E. Taylor and R. K. Skogerboe, Appl. Spectrosc. 33, 451 (1979).
2. G. F. Larson, V. A. Fassel, R. K. Winge and R. N. Kniseley, Appl. Spectrosc. 30, 384 (1976).
3. R. K. Winge, V. J. Peterson and V. A. Fassel, Appl. Spectrosc. 33, 206 (1979).
4. P. W. J. M. Boumans, Spectrochim. Acta, Part B 31, 147 (1976).
5. V. Bojovic and A. Antic-Javanovic, Spectrochim. Acta, Part B 27, 385 (1972).
6. V. G. Mossotti, F. N. Abercrombie and J. A. Eakin, Appl. Spectrosc. 25, 331 (1971).
7. W. Snelleman, T. C. Rains, D. W. Yee, H. D. Cook and O. Menis, Anal. Chem. 42, 394 (1970).
8. C. T. J. Alkemade and J. M. W. Milatz, Appl. Sci. Res. 4B, 289 (1955).
9. J. A. Bowman, J. V. Sullivan and A. Walsh, Spectrochim. Acta, Part B 22, 205 (1966).
10. O. I. Matveev, N. A. Tolstikova and E. P. Cheremukhin, Zavod. Lab. 45, 724 (1979).
11. R. L. Cochran and G. M. Hieftje, Anal. Chem. 49, 98 (1977).
12. R. L. Cochran and G. M. Hieftje, Anal. Chem. 50, 791 (1978).
13. P. A. St. John, W. J. McCarthy and J. D. Winefordner, Anal. Chem. 39, 1495 (1969).
14. J. A. Dean and T. C. Rains, "Flame Emission and Atomic Absorption Spectrometry," Vol. II, Marcel Dekker, New York, NY, 1969, ch. 13.



TABLE 1

AES-SLM System Components and Operating ConditionsBurners and Flames

Sample burner	5 cm $N_2O/C_2H_2$ slot burner with counter-flow jet spray nebulizer (Instrumentation Laboratory, Inc., Wilmington, MA)
Modulating burner	10.5 cm air/ $C_2H_2$ slot burner with impinging bead nebulizer (Varian Techtron, Palo Alto, CA)
Gas Flow Rates	Sample flame $N_2O$ : 3 L/min $C_2H_2$ : 2 L/min Modulating flame air: 15 L/min $C_2H_2$ : 3 L/min
Gas Handling	Purified flame gases (Matheson Co., Joliet, IL) controlled by needle valves (Series M, Nupro Co., Cleveland, OH) monitored by calibrated rotameters (No. VFB, Dwyer Instruments, Inc., Michigan City, IN)
Solution uptake	Sample solution: 4 mL/min Modulating solution: 3 mL/min
Observation height	Approximately 1 cm above burner tops

Optics

Monochromator	EU 700 GCA/McPherson Instrument, (Acton, MA) 0.35 m Czerny-Turner mount, slit width dependent upon experiment (50, 100, 300 $\mu$ m)
Chopper	Half-and-half configuration, front-surface aluminum, 11.5-cm diameter, rotated at 30 Hz by synchronous motor

Plane Mirrors

Front-surface aluminum;  $M_1$  diameter - 2.5 cm,  $M_2$  diameter - 5.1 cm (Melles Griot, Irvine, CA)

Lenses

$L_1$  diameter - 4.5 cm, F.L. = 30 cm  
 $L_2$  diameter - 2.5 cm, F.L. = 7.5 cm  
Lens material Suprasil I (Melles Griot, Irvine, CA)

Beam Attenuator

NRC (Fountain Valley, CA) 50600 AV.1 variable circular attenuator, optical density 0.5 to 1.0  $\pm$  0.5 at 633 nm, with evaporated aluminum, diameter - 5 in.

Beam Combiner

Diameter - 2.5 cm (No. 6-1325n, Special Optics, Little Falls, NJ) approximately 30% T, 30% R between 200-400 nm

Detection

Photomultiplier

RCA 1P28, operated at 500 to 900 volts. Supplied by a Fluke model 415B high-voltage power supply

Reference Detector

2N577 photodarlington transistor wired in a common-collector configuration, triggered by chopped light from a 12-V tungsten flashlight bulb

Signal Processing

Photocurrent converted to a proportional voltage by a model 215 operational amplifier and sent to a model 220 lock-in amplifier via a model 210 A frequency-selective amplifier. Reference signal sent to the model 220 amplifier via another model 210A amplifier. All of the above powered by model 200 NIM BIN supply (Princeton Applied Research Corp., Princeton, NY). Typical time constant, 1-3 sec.

Recorder

Heath/Schlumberger strip chart type, operated at 10 V full scale.

#### FIGURE CAPTIONS

- Figure 1. Schematic diagram of the double-beam AES-SLM system. The rotating sector mirror also produces the reference signal for the lock-in amplifier. See Table I for details of components. Radiation leaving this system falls on the entrance slit of the monochromator. The system's overall length is about 40 cm. The distance between beam paths is about 10 cm. See experimental section for further details.
- Figure 2. The effect of modulating solution concentration on barium (553.5 nm) analytical curves. Concentration of Ba in modulating solution: (A) 10,000  $\mu\text{g/mL}$ ; (B) 1000  $\mu\text{g/mL}$ ; (C) 500  $\mu\text{g/mL}$ ; (D) 200  $\mu\text{g/mL}$ ; (E) 100  $\mu\text{g/mL}$ . Monochromator spectral slit width = 0.6 nm.
- Figure 3. Determination of optimal modulating concentrations for barium (553.5 nm). The sample solution contains 50  $\mu\text{g/mL}$  Ba. Spectral slit width = 0.6 nm.
- Figure 4. Reduction of CaOH spectral interference on barium resonance line (553.5 nm). (A) Emission scan of 10  $\mu\text{g/mL}$  Ca and 20  $\mu\text{g/mL}$  Ba. (B) SLM scan of the same sample, using 1000  $\mu\text{g/mL}$  Ba modulating solution.
- Figure 5. The effect of added calcium on the SLM detection of the barium resonance line (553.5 nm). Ba concentration is a constant

10  $\mu\text{g/mL}$ . (A) Without SLM; (B) With SLM, using 1000  $\mu\text{g/mL}$  Ba modulating solution. See text for details.

Figure 6. Reduction of palladium line interference on various nickel lines. Pd concentration = 250  $\mu\text{g/mL}$ , Ni concentration = 200  $\mu\text{g/mL}$ . (A) SLM scan using 1000  $\mu\text{g/mL}$  Ni modulating solution. (B) Conventional emission scan. Monochromator spectral slit width = 0.1 nm.

Figure 7. Reduction of flame background by SLM. (A) Conventional emission scan of  $\text{N}_2\text{O}/\text{C}_2\text{H}_2$  flame background. (B) SLM scan of the same flame with only solvent sprayed into the modulating flame.

Figure 1.

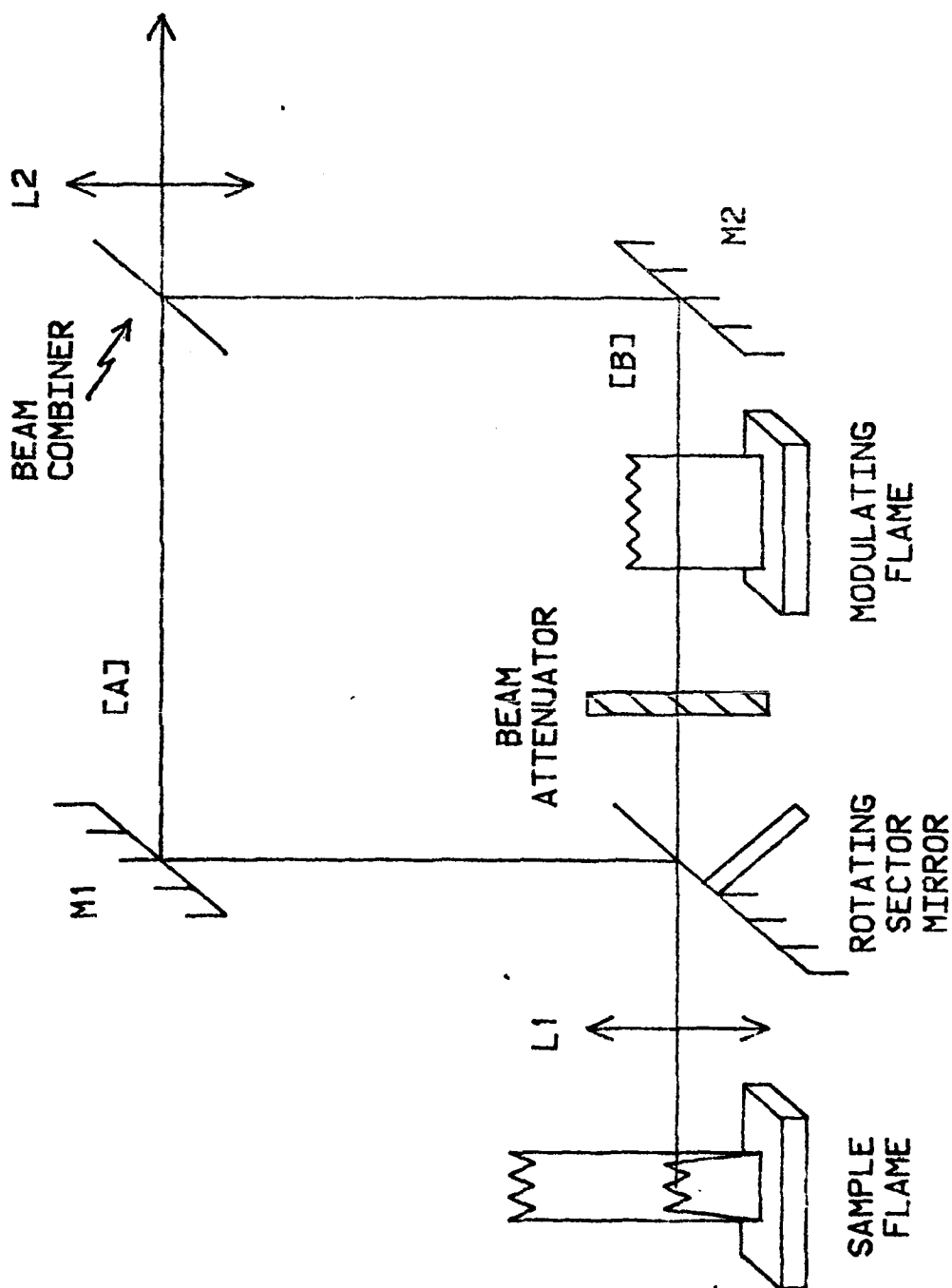


figure 2.

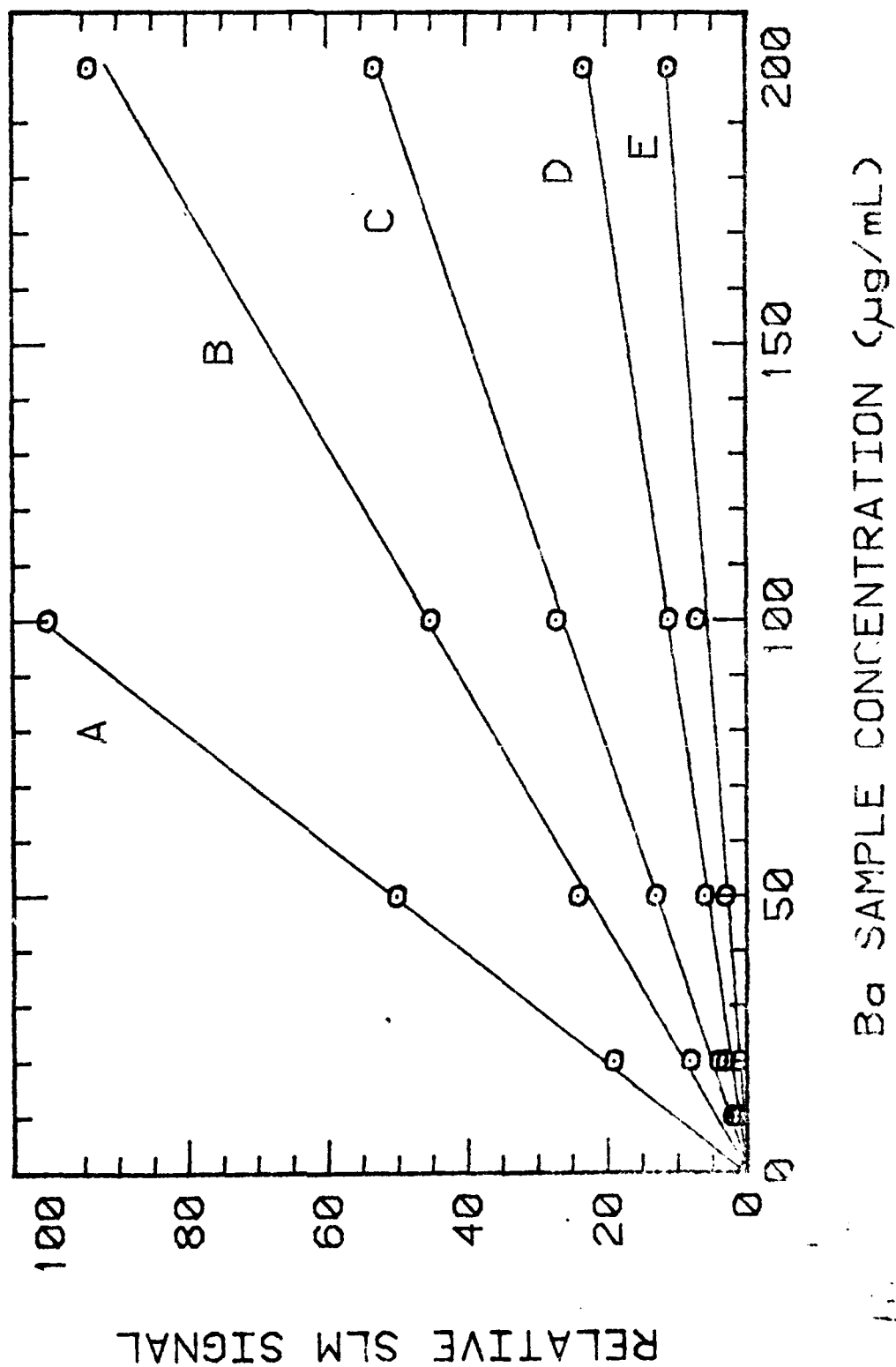
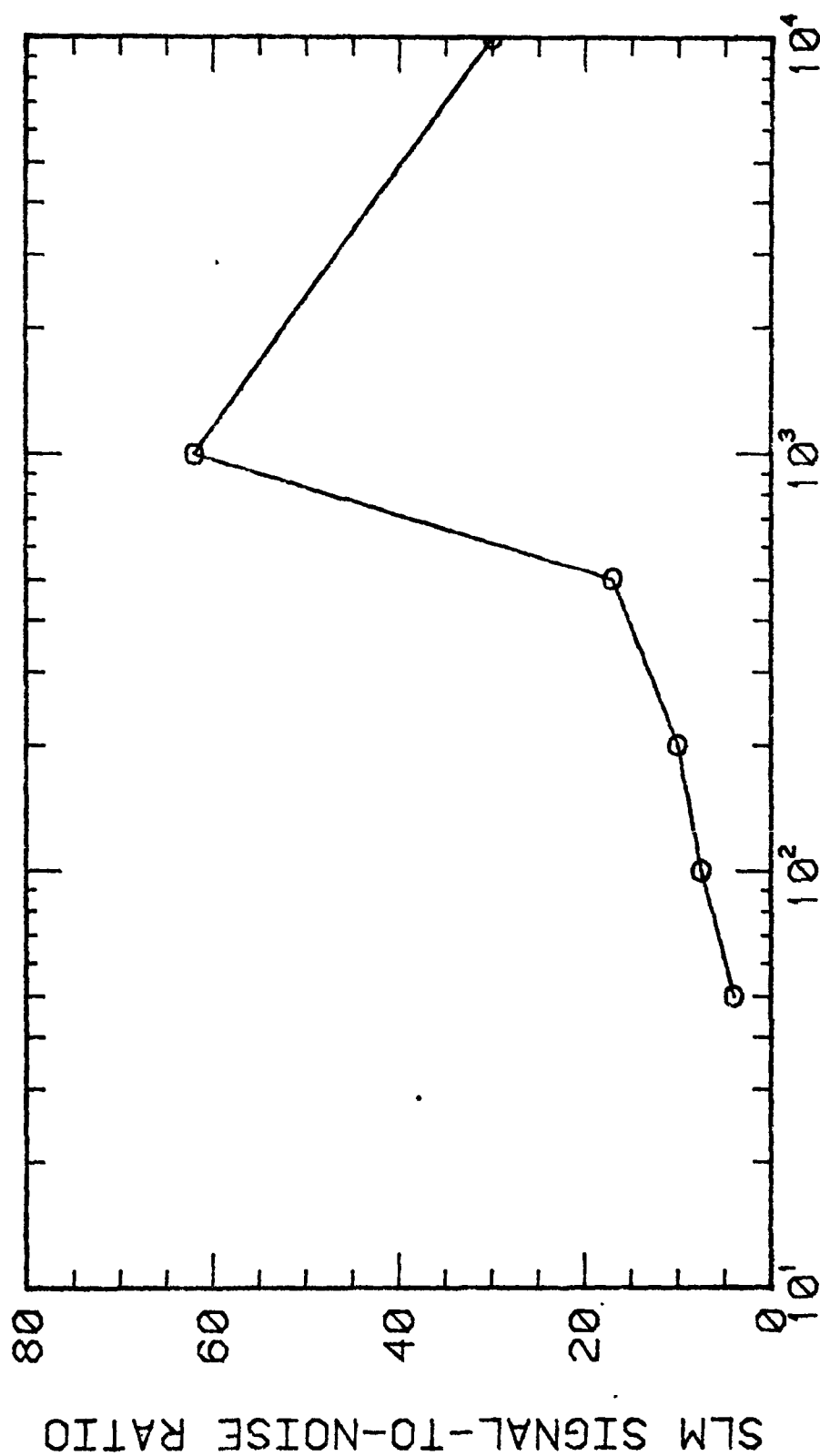


figure 3.



Ba MODULATING SOLUTION CONCENTRATION ( $\mu\text{g/mL}$ )

Figure 4.

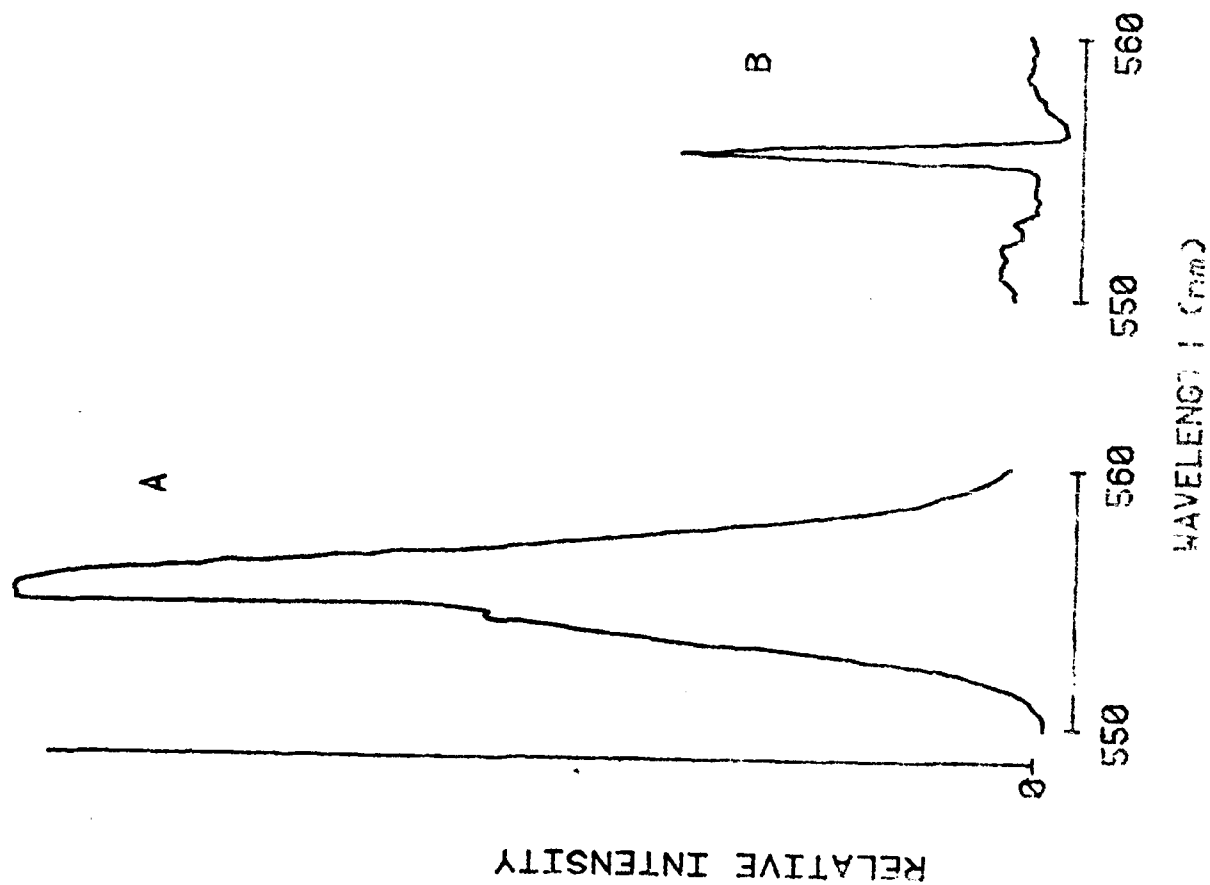
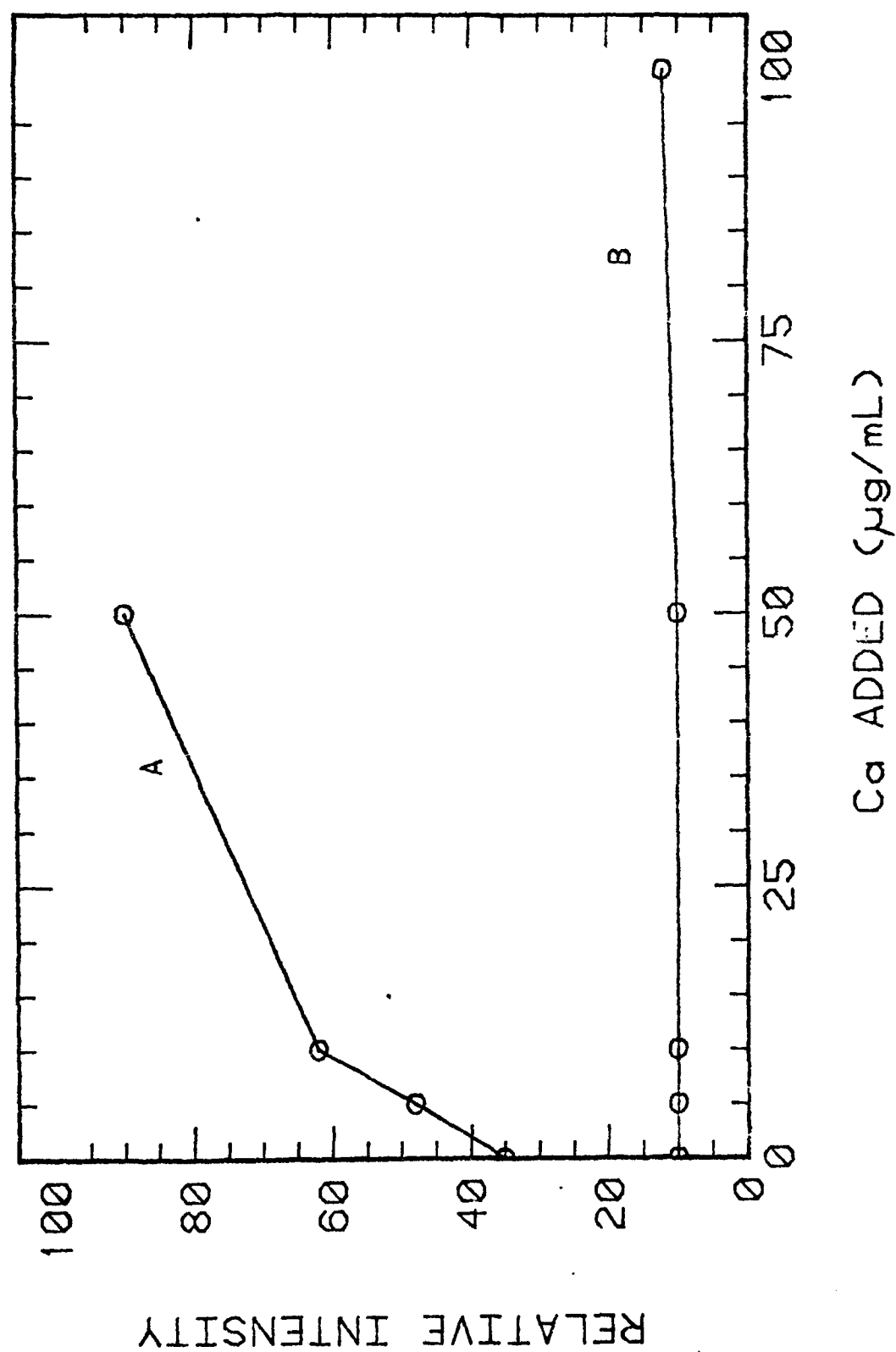
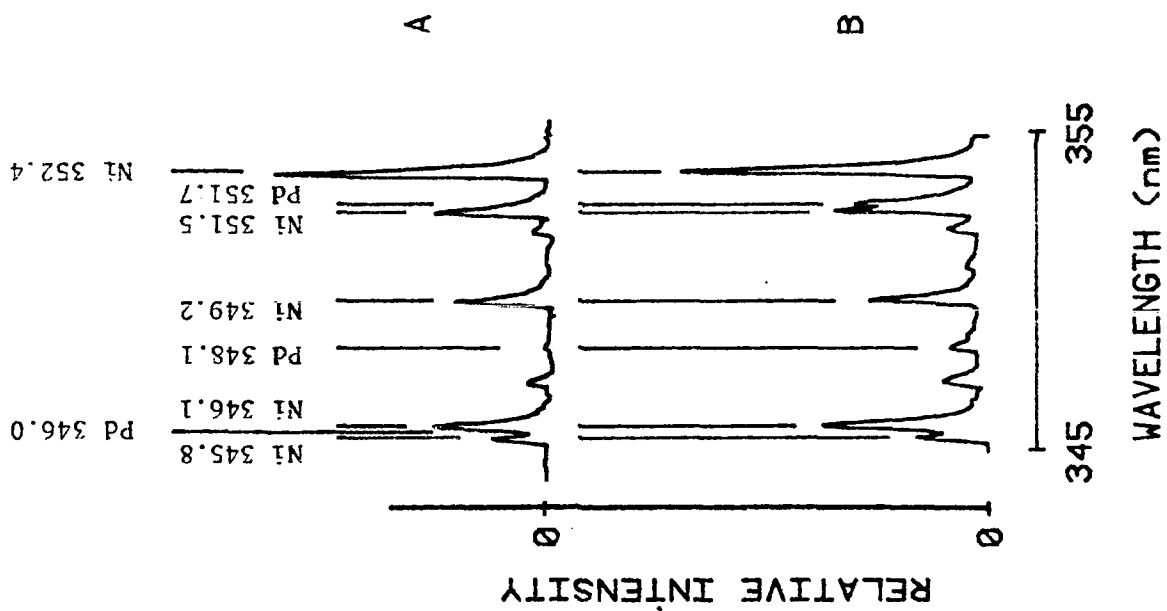


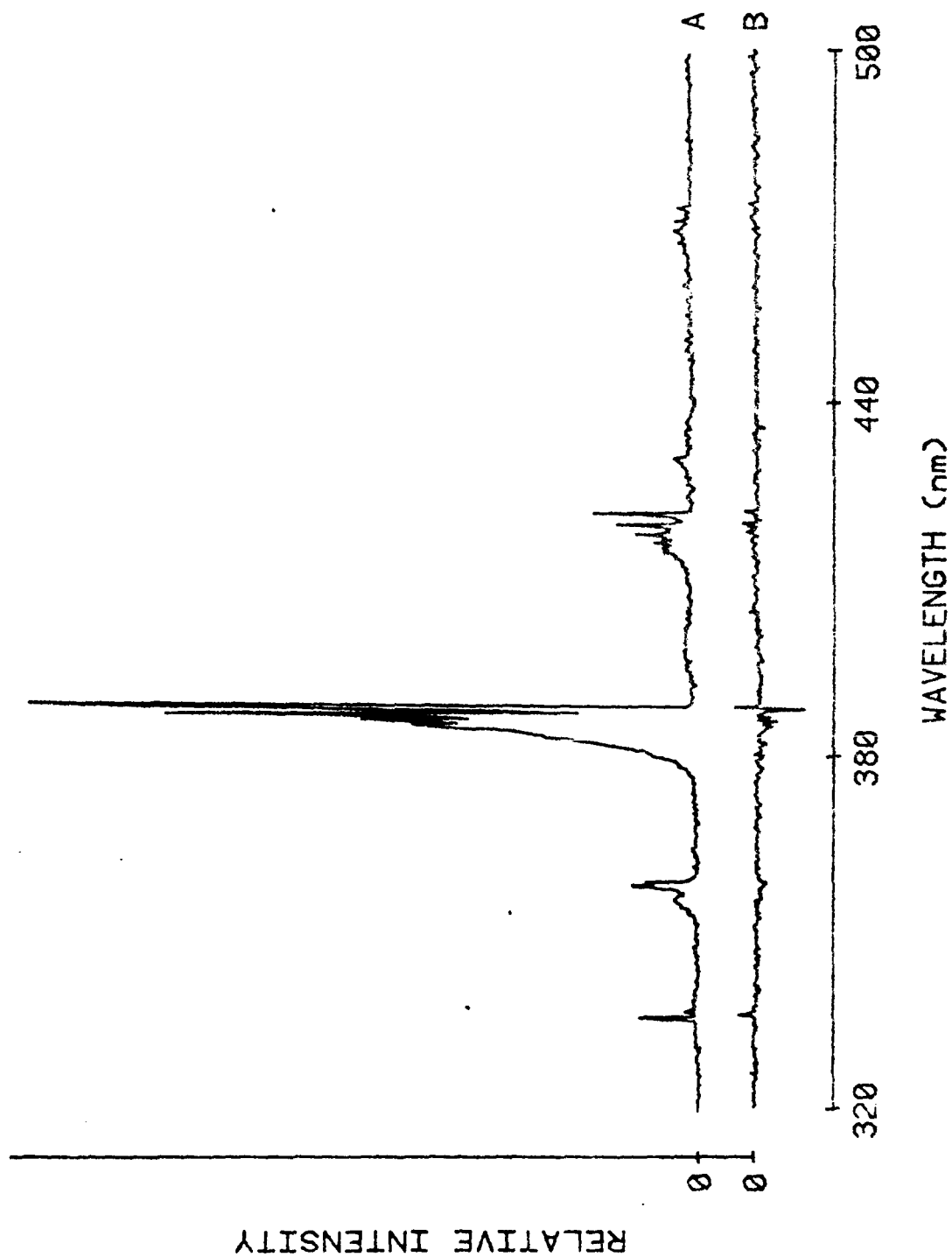


figure 5.





Figure



TECHNICAL REPORT DISTRIBUTION LIST, GEN

	<u>No. Copies</u>		<u>No. Copies</u>
Office of Naval Research Attn: Code 472 800 North Quincy Street Arlington, Virginia 22217	2	U.S. Army Research Office Attn: CRD-AA-IP P.O. Box 1211 Research Triangle Park, N.C. 27709	1
ONR Branch Office Attn: Dr. George Sandoz 536 S. Clark Street Chicago, Illinois 60605	1	Naval Ocean Systems Center Attn: Mr. Joe McCartney San Diego, California 92152	1
ONR Branch Office Attn: Scientific Dept. 715 Broadway New York, New York 10003	1	Naval Weapons Center Attn: Dr. A. B. Amster, Chemistry Division China Lake, California 93555	1
ONR Branch Office 1030 East Green Street Pasadena, California 91106	1	Naval Civil Engineering Laboratory Attn: Dr. R. W. Drisko Port Hueneme, California 93401	1
ONR Branch Office Attn: Dr. L. H. Peebles Building 114, Section D 566 Summer Street Boston, Massachusetts 02210	1	Department of Physics & Chemistry Naval Postgraduate School Monterey, California 93940	1
Director, Naval Research Laboratory Attn: Code 6100 Washington, D.C. 20390	1	Dr. A. L. Slafkosky Scientific Advisor Commandant of the Marine Corps (Code RD-1) Washington, D.C. 20380	1
The Assistant Secretary of the Navy (R,E&S) Department of the Navy Room 4E736, Pentagon Washington, D.C. 20350	1	Office of Naval Research Attn: Dr. Richard S. Miller 800 N. Quincy Street Arlington, Virginia 22217	1
Commander, Naval Air Systems Command Attn: Code 310C (H. Rosenwasser) Department of the Navy Washington, D.C. 20360	1	Naval Ship Research and Development Center Attn: Dr. G. Bosmajian, Applied Chemistry Division Annapolis, Maryland 21401	1
Defense Documentation Center Building 5, Cameron Station Alexandria, Virginia 22314	12	Naval Ocean Systems Center Attn: Dr. S. Yamamoto, Marine Sciences Division San Diego, California 91232	1
Dr. Fred Saalfeld Chemistry Division Naval Research Laboratory Washington, D.C. 20375	1	Mr. John Boyle Materials Branch Naval Ship Engineering Center Philadelphia, Pennsylvania 19112	1

TECHNICAL REPORT DISTRIBUTION LIST, 051C

	<u>No. Copies</u>		<u>No. Copies</u>
Dr. M. B. Denton Department of Chemistry University of Arizona Tucson, Arizona 85721	1	Dr. John Duffin United States Naval Postgraduate School Monterey, California 93940	1
Dr. R. A. Osteryoung Department of Chemistry State University of New York at Buffalo Buffalo, New York 14214	1	<del>Dr. G. M. Hieftje Department of Chemistry Indiana University Bloomington, Indiana 47401</del>	1
Dr. B. R. Kowalski Department of Chemistry University of Washington Seattle, Washington 98105	1	Dr. Victor L. Rehn Naval Weapons Center Code 3813 China Lake, California 93555	1
Dr. S. P. Perone Department of Chemistry Purdue University Lafayette, Indiana 47907	1	Dr. Christie G. Enke Michigan State University Department of Chemistry East Lansing, Michigan 48824	1
Dr. D. L. Venezky Naval Research Laboratory Code 6130 Washington, D.C. 20375	1	Dr. Kent Eisentraut, MBT Air Force Materials Laboratory Wright-Patterson AFB, Ohio 45433	1
Dr. H. Freiser Department of Chemistry University of Arizona Tucson, Arizona 85721		Walter G. Cox, Code 3632 Naval Underwater Systems Center Building 148 Newport, Rhode Island 02840	1
Dr. Fred Saalfeld Naval Research Laboratory Code 6110 Washington, D.C. 20375	1	Dr. Rudolph J. Marcus Office of Naval Research Scientific Liaison Group American Embassy APO San Francisco 96503	
Dr. H. Chernoff Department of Mathematics Massachusetts Institute of Technology Cambridge, Massachusetts 02139	1	Mr. James Kelley DTNSRDC Code 2803 Annapolis, Maryland 21402	
Dr. K. Wilson Department of Chemistry University of California, San Diego La Jolla, California	1		
Dr. A. Zirino Naval Undersea Center San Diego, California 92132	1		